# Apohorseradish Peroxidase Unfolding and Refolding: Intrinsic Tryptophan Fluorescence Studies

Mauricio Lasagna,* Enrico Gratton,# David M. Jameson,§ and Juan E. Brunet*

*Instituto de Química, Universidad Católica de Valparaiso, Casilla 4059, Valparaiso, Chile; #Laboratory for Fluorescence Dynamics, Physics Department, University of Illinois at Urbana-Champaign, Urbana, Illinois 61801 USA; and §Department of Genetics and Molecular Biology, University of Hawaii, Honolulu, Hawaii 96822 USA

ABSTRACT The unfolding and refolding of apohorseradish peroxidase, as a function of guanidinium chloride concentration, were monitored by the intrinsic fluorescence intensity, polarization, and lifetime of the single tryptophan residue. The unfolding was reversible and characterized by at least three distinct stages—the intensity and lifetime data, for example, were both characterized by an initial increase followed by a decrease and then a plateau region. The lifetime data, in the absence and presence of guanidinium chloride, were heterogeneous and fit best to a model consisting of a major Gaussian distribution component and a minor, short discrete component. The observed increase in intensity in the initial stage of the unfolding process is attributed to the conversion of this short component into the longer, distributed component as the guanidinium chloride concentration increases. Our results clarify and amplify previous studies on the unfolding of apohorseradish peroxidase by guanidinium chloride.

## INTRODUCTION

Horseradish peroxidase (donor:hydrogen-peroxidase oxidoreductase, EC 1.11.1.7) (HRP) is a member of the important group of plant peroxidases that catalyze the oxidation and peroxidation of a variety of organic and inorganic compounds. A number of acidic, neutral, and basic isoenzymes of HRP have been identified and classified (Shannon et al., 1966; Paul and Stigbrand, 1970; Delincee and Radolla, 1970; Bartonek-Roxå et al., 1991). HRP-C is a monomeric glycoprotein of molecular weight 44,000 with eight N-linked carbohydrate chains and one noncovalently bound hemin moiety (Clarke and Shannon, 1976; Welinder, 1979, 1985).

The unfolding and refolding of HRP, with and without the heme moiety, are of general interest to those studying protein denaturation and renaturation and are of specific interest to those interested in the expression of recombinant HRP (Smith et al., 1990; Hartman and Ortiz de Montellano, 1992; Bartonek-Roxå and Eriksson, 1994; Moosavi-Movajedi and Nazari, 1995). Fluorescence spectroscopy has been widely applied to the study of protein folding (see, for example, James et al., 1992; Eftink, 1994; Watanabe et al., 1996; Jiskoot et al., 1995). In the case of HRP, both intrinsic and extrinsic fluorescent probes have been utilized for this purpose. Extrinsic probes utilized include 1-anilino-8-naphthalene sulfonate (ANS), 4,4′-bis(1-anilino-8-naphthalene sulfonate (bis-ANS), 2-*p*-toluidiny-6-naphthalene sulfonate (TNS), and protoporphyrin IX (PPIX), which bind to and monitor the heme binding site (Ugarova et al., 1981; Jullian et al., 1989; Vargas et al., 1991; Brunet et al., 1994). HRP's single tryptophan residue (W117) also serves as an intrinsic probe that can monitor another region of the protein. Although the x-ray structure of HRP is not yet available, fluorescence energy transfer studies indicate that the tryptophan residue is between 12 and 18 Å from the heme binding site (Brunet et al., 1983; Ohlsson et al., 1986; Pappa and Cass, 1993; Das and Mazumdar, 1995). Hence, by monitoring the intrinsic tryptophan fluorescence as well as the fluorescence of probes associated with the heme binding site one can, in principle, follow the effects of denaturants on two distinct regions of the protein.

Recently, Pappa and Cass (1993), motivated by an interest in understanding the refolding of recombinant protein isolated from inclusion bodies, described fluorescence and circular dichroism (CD) measurements on the guanidinium chloride-induced unfolding and refolding of both holo- and apoHRP. They found that their fluorescence intensity results on apoHRP could be fit to a two-stage transition, whereas their CD results (based on both 278 nm and 222 nm observations) suggested a more complex unfolding pattern. They also suggested that PPIX associated with apoHRP exhibited considerable local motion, indicating a loose association with the heme binding site, and that it did not stabilize the protein structure as well as hemin. Our previous results on dynamic aspects of apoHRP-PPIX and our recent studies on the guanidinium chloride-induced unfolding of apoHRP prompted us to reevaluate some of the conclusions of Pappa and Cass. To this end we utilized both steady-state (including polarization) and time-resolved fluorescence measurements on the intrinsic fluorescence of apoHRP. Our results led us to conclude that there are, in fact, at least two spectroscopically distinct forms of apoHRP in the absence of GuHCl and that the distinction begins to disappear immediately upon the addition of denaturant, well before the overall collapse of the native structure, which occurs at

*Received for publication 20 April 1998 and in final form 11 September 1998.*

Address reprint requests to Dr. Juan Brunet, Instituto de Química, Universidad Católica de Valparaiso, Casilla 4059, Valparaiso, Chile. Tel.: 56-32-222557; Fax: 56-32-212746; E-mail: jbrunet@u.c.v.cl.



0006-3495/99/01/443/08 $2.00

higher denaturant concentrations. This conclusion, based on lifetime results, cannot be reached by the observations of steady-state intensities carried out by Pappa and Cass.

## MATERIAL AND METHODS

### Preparation of ApoHRP

Boehringer Mannheim EL grade HRP, which contains isoenzyme C as the major component, was utilized without further purification. The apoHRP was prepared by removing the heme group according to Teale's method (Teale, 1959) of cold acid and butanone extraction followed by exhaustive dialysis at 4°C against 0.1 M sodium phosphate buffer at pH 7.4. The concentration of apoHRP was determined by absorption spectrophotometry, using a molar extinction coefficient of 20,000 $M^{-1}$ $cm^{-1}$ at 280 nm (Tamura et al., 1972).

### Unfolding/refolding protocols

For the denaturation experiments guanidinium chloride from an 8.0 M stock solution was used, and appropriate protein aliquots from a protein stock solution were added to the desired concentration of denaturant such that the final protein concentration was $5.0 \times 10^{-6}$ M. Spectral measurements were taken 24 h after introduction of the denaturant. The renaturation experiments were performed by dissolving the protein in 8.0 M guanidinium chloride, followed by a 24-h incubation period, readjustment of the denaturant concentration, and then another 24-h incubation period before the fluorescence measurements were performed. Because reducing reagents are not added during unfolding or refolding experiments, the four disulfide bonds of apoHRP remain intact.

### Steady-state fluorescence

Uncorrected fluorescence spectra were obtained with a SPEX Fluorolog photon counting spectrofluorimeter updated with ISS (ISS, Champaign, IL) acquisition electronics and software. The total fluorescence intensity and the polarization measurements were obtained on a Greg 200 spectrofluorometer (ISS). Spectral bandwidths of 2 nm were used for all measurements, and all signals were corrected for buffer blanks. For the total intensity measurements on the intrinsic fluorescence, the proteins were excited at 295 nm and emission at wavelengths greater than 305 nm was viewed through a Schott WG 315 cut-on filter. The polarization measurements were performed using 300-nm excitation and viewing emission at wavelengths greater than 325 nm through a Schott WG 335 cut-on filter. The total fluorescence intensity, obtained upon excitation with parallel polarized light, was obtained as $I_T = I_\parallel + 2I_\perp$, where $I_\parallel$ and $I_\perp$ are the intensities observed through polarizers oriented, respectively, parallel and perpendicular to the laboratory axis.

### Time-resolved fluorescence

Time-resolved measurements were obtained using a laser-based instrument at the Laboratory for Fluorescence Dynamics (LFD) at the University of Illinois at Urbana-Champaign. In this laser-based instrument, the frequency modulation of the excitation source is realized using the harmonic content approach (Gratton et al., 1984; Alcala et al., 1985). The exciting light was from a Coherent Nd:YAG mode-locked laser pumping a rhodamine dye laser. The dye laser was tuned to 590 nm, which was then frequency doubled to 295 nm. Emission was observed through a Schott WG320 filter to isolate the emission of tryptophan and to block scattered light. The exciting light was polarized parallel to the vertical laboratory axis, and the emission was viewed through a polarizer oriented at 55° to eliminate polarization effects on the lifetime measurements (Spencer and Weber, 1970). The reference fluorophore used was *p*-terphenyl in ethanol with a lifetime of 1.05 ns. Phase and modulation values for the lifetime data were obtained as previously described (Spencer and Weber, 1969; Jameson et al., 1984; Jameson and Hazlett, 1991). The lifetime data were analyzed either by assuming a sum of discrete exponentials (Jameson et al., 1984) or by using continuous distribution models that assumed either Lorentzian or Gaussian distributions (Alcala et al., 1987a,b,c).

## RESULTS

### Intensity and spectral measurements

Fig. 1 shows the unfolding and the refolding of apoHRP in the presence of varying concentrations of guanidinium chloride as monitored by the total fluorescence intensity upon

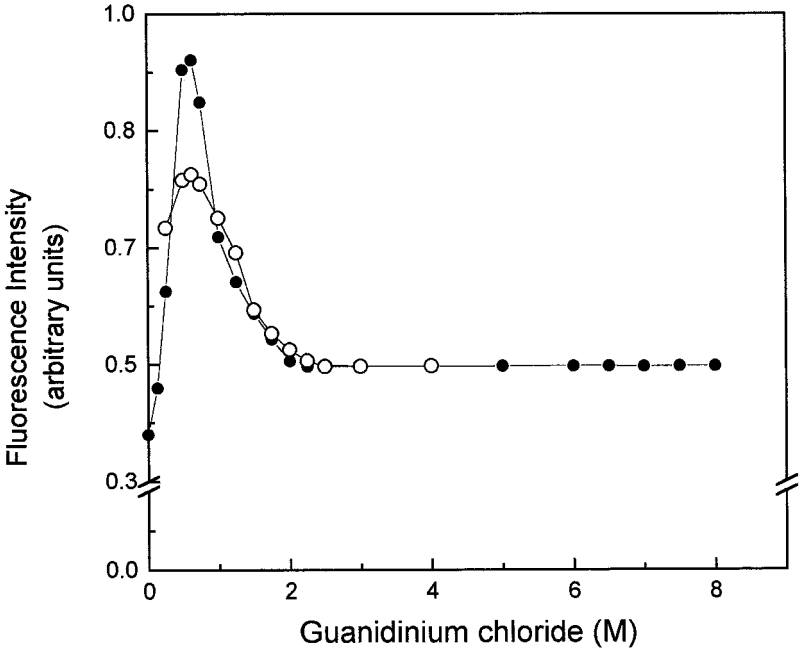


FIGURE 1 Total fluorescence intensity for apoHRP as a function of guanidinium chloride concentration at 20°C: unfolding (●) and refolding (○).

295-nm excitation. The unfolding pathway, monitored in this fashion, exhibits an increase in the emission intensity reaching a maximum at ~0.6 M guanidinium chloride followed by a decrease, and then a stabilization at an intensity slightly higher than the initial value. The unfolding and folding curves follow nearly the same path, indicative of a reversible process, although the maximum intensity observed on the folding pathway (near 0.6 M) is less than that observed on the unfolding pathway. Fig. 2 shows the effect of guanidinium chloride concentration on the emission maximum of apoHRP. The maximum in the absence of denaturant is 343 nm and increases immediately upon the addition of guanidinium chloride, with a small plateau appearing near 0.6 M, finally leveling off at 356 nm near 4 M denaturant.

## Polarization measurements

The effects of guanidinium chloride on the polarization of apoHRP are shown in Fig. 2. Excitation at 300 nm was used for these unfolding and refolding polarization experiments, because this wavelength does not excite tyrosine residues and avoids the complication of tyrosine-to-tryptophan energy transfer. The unfolding pathway, monitored in this fashion, shows a generally monotonic decrease in polarization as a function of denaturant concentration, with slight but reproducible changes in slopes at ~0.6 M, ~2 M, and ~4 M guanidinium chloride. The polarization values along the refolding pathway closely follow those of the unfolding pathway (data not shown). The excitation polarization spectrum for apoHRP in 0.1 M, pH 7.4 phosphate buffer at 20°C is shown in the inset in Fig. 2. The data show the characteristic features associated with proteins containing tyrosine and tryptophan residues (Weber, 1960). The ratio of the polarizations observed upon excitation at 300 nm relative to 270 nm is high (1.92), indicative of significant tyrosine-to-tryptophan energy transfer (Weber, 1960). Tryptophan in a rigid medium, for example, exhibits a 300/270 ratio near 1.45.

## Lifetime measurements

The lifetime data for apoHRP were indicative, in all cases, of heterogeneous decay, i.e., in the presence or absence of denaturant, phase and modulation data could not be fit to a single-exponential model. Table 1 shows, for example, fits of the lifetime data for apoHRP at 0.5 M guanidinium chloride, to single, double, and triple discrete exponential decays, as well as to Lorentzian and Gaussian distribution models. The data were well fit to a predominant Gaussian component and a small fraction of a discrete component (0.35 ns). Fig. 3 shows the Gaussian distributions for apoHRP in 0 M, 0.5 M, and 7.6 M guanidinium chloride. Fig. 4 shows the variation of the center and the width of the Gaussian distributions and the fractional contribution of the discrete component as a function of guanidinium chloride concentration. One notes that the center value of the distribution increases immediately upon the addition of the denaturant and goes from ~3.3 ns at 0 M to 3.9 ns near 0.6 M guanidinium chloride. Concomitantly, the fraction attributed to the short, discrete component decreases steadily as the denaturant concentration increases (Fig. 4, *inset*) and disappears near 0.5 M denaturant (these data were analyzed by global analysis, wherein the lifetime of the discrete component was linked throughout the data sets but all other parameters were free to vary). Fig. 4 also shows the center values for the distributions obtained for apoHRP upon dilution of the denaturant.

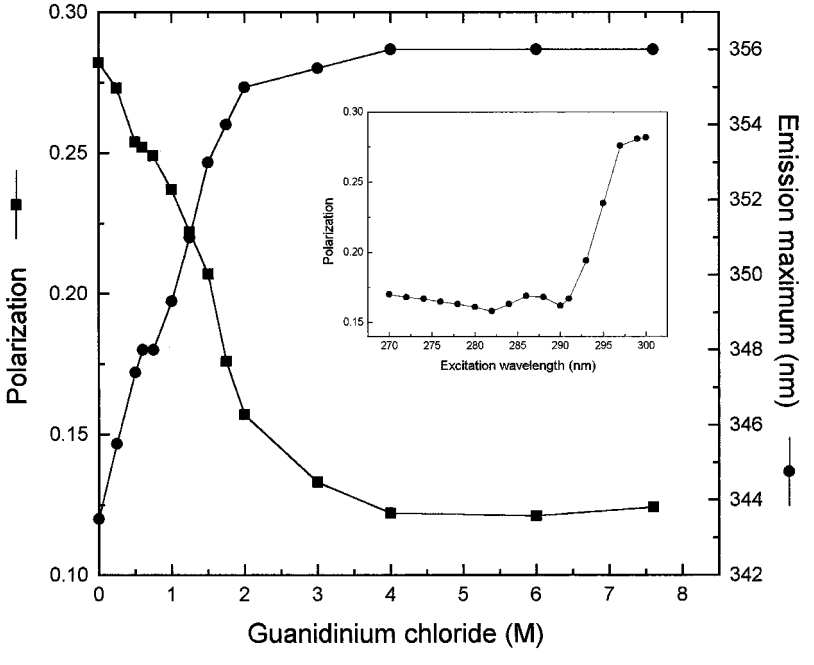


FIGURE 2 ApoHRP emission maximum (●) and polarization (■) as a function of guanidinium chloride concentration at 20°C. Inset shows the excitation polarization spectrum for apoHRP.

**TABLE 1 Lifetime data for apoHRP in 0.5 M guanidinium chloride fit to various models**

| Discrete exponentials | | | | | | |
|---|---|---|---|---|---|---|
| $\tau_1$ | $f_1$ | $\tau_2$ | $f_2$ | $\tau_3$ | $f_3$ | $\chi^2$ |
| 3.08 | 1.00 | — | — | — | — | 576 |
| 4.50 | 0.82 | 0.90 | 0.18 | — | — | 11.7 |
| 5.53 | 0.59 | 2.10 | 0.36 | 0.41 | 0.05 | 0.41 |
| Lorentzian | | | | | | |
| $\tau_1$ | Width | $f_1$ | $\tau_2$ | $f_2$ | | $\chi^2$ |
| 3.90 | 1.54 | 0.93 | 0.68 | 0.07 | | 2.70 |
| Gaussian | | | | | | |
| $\tau_1$ | Width | $f_1$ | $\tau_2$ | $f_2$ | | $\chi^2$ |
| 3.87 | 2.21 | 0.999 | 0.35 | 0.001 | | 0.23 |

$\tau$'s represent lifetime values in nanoseconds, $f$'s represent fractional intensity contributions, width refers to the full width at half-maximum, and $\chi^2$ represents the reduced chi-squared value for the fit assuming errors of 0.2° and 0.004 for phase and modulation data, respectively.

## DISCUSSION

The fluorescence intensity versus denaturant curves we obtained (Fig. 1) were roughly similar to those of Pappa and Cass (1993) but differed in the ratio of the intensities corresponding to the maximum value (at ~0.6 M guanidinium chloride) and the value observed at the maximum denaturant concentration. Specifically, the ratio we observed for these values was nearly 2, whereas that obtained by Pappa and Cass (1993) was close to 1.2. Pappa and Cass also reported that the initial increase in intensity upon the addition of guanidinium chloride exhibited a sigmoidal shape, which they stated was characteristic of a simple two-state transition. Our results, however, did not show such sigmoidal behavior. These differences are due to the methodology utilized by Pappa and Cass. Specifically, Pappa and Cass observed the emission intensity at 350 nm, upon 290-nm excitation, as a function of denaturant concentration. In the case of HRP, this approach is problematic for two reasons: 1) 290 nm will excite some tyrosine fluorescence (which will, according to our excitation polarization results (*vide supra*), transfer energy to the tryptophan moiety) and, more importantly, 2) the emission maximum changes upon the addition of denaturant, and consequently observation at a fixed emission wavelength will immediately lead to apparent shifts in intensity not related to the actual quantum yield. For these reasons we employed 295-nm excitation to minimize excitation of tyrosine residues, and, more importantly, we observed the total fluorescence intensity through a cut-on filter by exciting with parallel light and determining the total intensity function, $I_T = I_{\parallel} + 2I_{\perp}$, where $I_{\parallel}$ and $I_{\perp}$ are the intensities observed through polarizers oriented, respectively, parallel and perpendicular to the laboratory axis. This method has the additional advantage that it avoids systematic errors in observed intensities, which can arise in two ways when there are changes in polarization: 1) preferential response of the monochromator/detector system to one plane of polarization (Jameson, 1984) and 2) the intrinsic bias introduced by a right angle observation geometry (Spencer and Weber, 1970). We note that this approach works well when the quantum yield of the system changes; however, in some cases the more rigorous approach of collecting the complete, corrected emission spectra associated with the parallel and perpendicular components, followed by reconstruction of the "total emission spectrum," may be warranted. One notes from the lifetime results (Fig. 4) that the maximum lifetime value reached on the refolding path was the same as that observed on the unfolding path, i.e., near 3.9 ns. These results indicate that the decreased intensity observed on the refolding path relative to the unfolding path (Fig. 1) may be due to loss of some material, via aggregation for example, which would affect intensity measurements but not lifetime values.

The excited-state decays of a number of single tryptophan-containing proteins have been analyzed in terms of continuous lifetime distribution models (Alcala et al., 1987a,b,c; Gratton et al., 1992; Silva et al., 1994). Distributional models are characterized by two parameters: the center lifetime value and the width, i.e., full width at half-maximum. The distributional approach to analyzing lifetime data is based on the assumption that multiple protein conformational substates exist and that the dynamics of interconversion between these states affects the observed lifetime (Silva et al., 1994). Our lifetime results demonstrate that the excited-state kinetics exhibited by the tryptophan in the apoHRP, in the absence or presence of the denaturant, cannot be well fit, as judged by the reduced $\chi^2$ value (Table 1), to one or two discrete decay components. However, the lifetime data can be fit well to a single Gaussian distributional component plus a small fraction of a short, discrete component, at denaturant concentrations below ~0.5 M, and to a single Gaussian distribution at denaturant concentrations above ~0.5 M. These data also indicate that the width of the lifetime distribution increased slightly as the concentration of denaturant increased to ~1.0 M guanidinium chloride, at which point the width decreased mark-

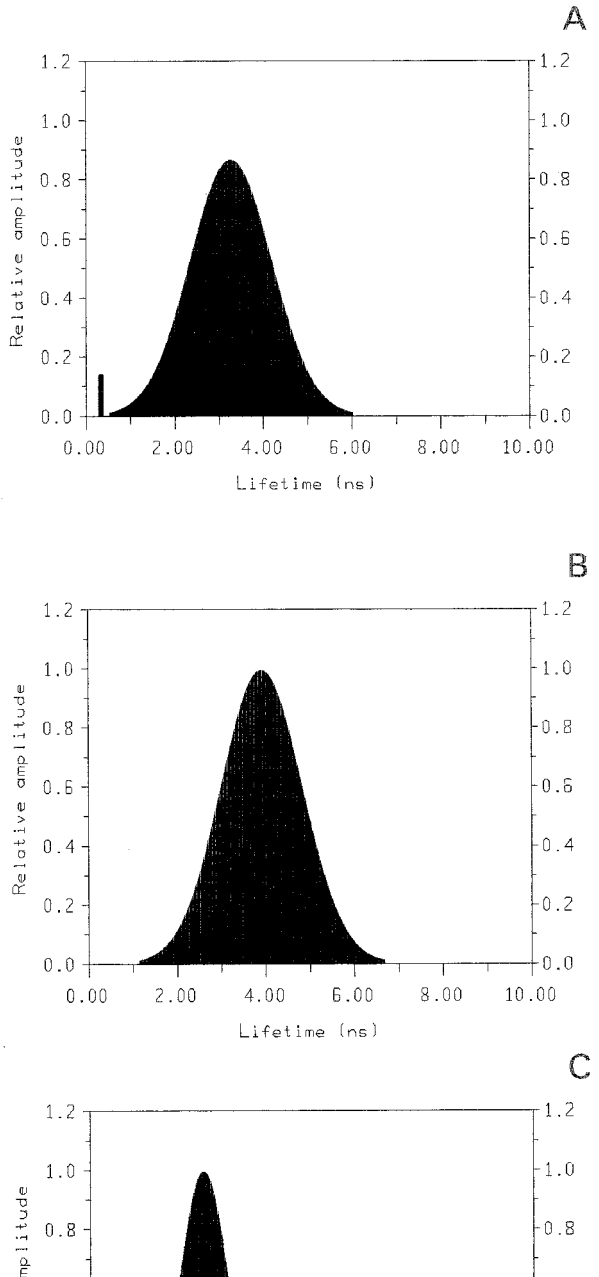


FIGURE 3 Gaussian distribution curves corresponding to the lifetime results for apoHRP in 0 M (*A*), 0.5 M (*B*), and 7.6 M (*C*) guanidinium chloride.

edly, reaching a value at the maximum denaturant concentration significantly lower than that in the absence of denaturant. This result is notably different from similar studies on tuna apomyoglobin (Bismuto et al., 1988) and human superoxide dismutase (Mei et al., 1992). In the apomyoglobin case the data fit best to a Lorentzian distribution, and the width of this distribution increased dramatically above 0.5 M guanidinium chloride, remaining constant above ~2 M denaturant. In the human superoxide dismutase case there was a significant initial increase in the width of the distribution, followed by a slight decrease at higher denaturant concentration, but the width at the highest denaturant concentration was significantly larger than that in the absence of denaturant. Our lifetime results on apoHRP suggest that either the number of conformational substates available for the tryptophan in the unfolded protein is less than in native protein or that the dynamics of the interconversion between substates is enhanced in unfolded apoHRP. The fact that unfolded apoHRP still has four disulfide bonds in our denaturation conditions may, in fact, limit the conformational substates accessible. One may expect that the ratio of the lifetimes at zero and 0.6 M guanidinium chloride would match the corresponding ratio of the intensities. The intensity ratio, however, is 2.45, whereas the ratio of the long-lifetime components is 3.94/3.34 = 1.18. A more appropriate calculation should take the short component into account. The initial intensity increase, in fact, can be more reasonably accounted for if the short, discrete component is converted into the longer, distributed component as guanidinium chloride is added. Specifically, if we consider the intensity ($I$) in the absence of denaturants to be due to two components, a "long" component ($\tau_1$) and a "short" component ($\tau_2$), then

$$I = \alpha_1\tau_1 + \alpha_2\tau_2$$

where $\alpha_1$ and $\alpha_2$ are preexponential factors. The relationships between the preexponential factors and the fractional contributions to the steady-state intensities ($f_i$) are given by

$$\alpha_1 = \frac{\left(\frac{f_1}{\tau_1}\right)}{\left(\frac{f_1}{\tau_1}\right) + \left(\frac{f_2}{\tau_2}\right)}; \quad \alpha_2 = \frac{\left(\frac{f_2}{\tau_2}\right)}{\left(\frac{f_1}{\tau_1}\right) + \left(\frac{f_2}{\tau_2}\right)}$$

In the absence of denaturant, $\tau_1 = 3.34$ (using the center value of the distribution), $f_1 = 0.862$, $\tau_2 = 0.35$, and $f_2 = 0.138$, which results in $\alpha_1 = 0.40$ and $\alpha_2 = 0.60$. The normalized intensities at zero and 0.6 M guanidinium chloride are thus $I_0 = (0.60)(0.35) + (0.40)(3.34) = 1.55$ and $I_{0.6M} = (0)(0.35) + (1.0)(3.94) = 3.94$. The ratio of these calculated intensities is thus 2.54, compared to 2.45, the ratio of the observed intensities. This calculation is admittedly not strictly correct, because it should be used only for discrete components, and we are using the center value of a distribution for one component, but the purpose of the calculation is to demonstrate the principle involved and to show that the apparent discrepancy between the observed intensity and lifetime ratios for zero and 0.6 M denaturant can be accounted for, in principle, with a simple model.

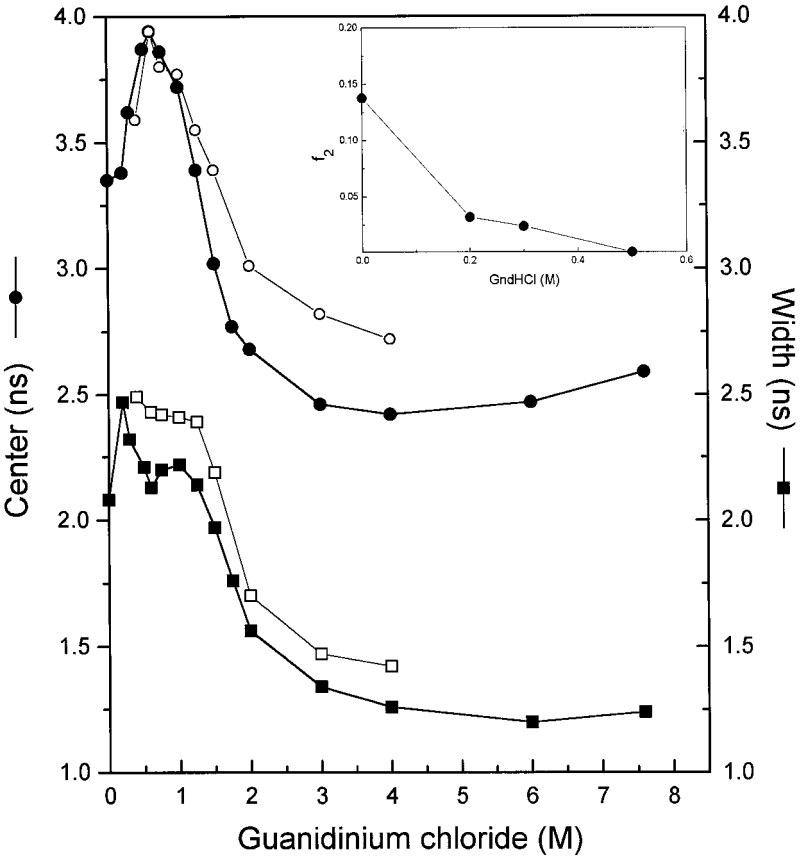


FIGURE 4 Center value (●) and width (■) corresponding to the Gaussian distribution fits for apoHRP as a function of guanidinium chloride concentration. Closed symbols refer to the unfolding path, and open symbols refer to the refolding path. Inset shows the fractional contribution associated with the short, discrete component (0.35 ns) as a function of guanidinium chloride concentration.

Furthermore, if the short, discrete component has an emission maximum blue-shifted with respect to the major component, the disappearance of this short component coupled with its reappearance as a red-shifted component would also account for the observed red shift in the emission spectrum in the 0–0.6 M denaturant range. Similarly, the initial decrease in the polarization could be due to the disappearance of this shorter-lived component, which would be expected to have a higher polarization value as a consequence of its shorter lifetime. In fact, using the Perrin equation, the polarization change from 0.282 (at zero denaturant) to 0.252 (at 0.6 M denaturant) can be almost quantitatively accounted for by the increase in the "average" lifetime from 2.93 ns (at zero denaturant) to 3.94 ns (at 0.6 M denaturant), assuming that the average rotational relaxation time of the protein does not vary over this denaturant range. This result suggests that mobility of the tryptophan residue does not change significantly in the 0–0.6 M denaturant range.

Smith et al. (1990) pointed out in their studies on recombinant HRP that the protein needs an excess of calcium to stabilize a conformation suitable for accepting the prosthetic group and that the renaturation of HRP is not a reversible process. Renaturation of apoHRP, on the other hand, appears to be reversible and to involve more than two states. The intensity data show an intermediate state that reaches an intensity maximum near 0.6 M guanidinium chloride. The presence of this intermediate state is also apparent in the denaturation and renaturation curves after the polarization of the tryptophan residue, as shown in Fig. 2. The attribution of this intermediate state to a molten globule cannot be made with certainty, however, especially because the usual approach of studying ANS binding is precluded in this case, because ANS binds well to the heme-binding site region (Vargas et al., 1991).

Our data are generally in agreement with the conclusions of Pappa and Cass (1993) based on their CD experiments, i.e., that unfolding of apoHRP occurs through a process with at least three states, as was suggested by the fact that their denaturation curve from the backbone CD did not coincide with that from the aromatic CD. Our CD results (data not shown) completely support these observations. The lack of agreement between the backbone and aromatic CD results is indicative of a change in the tertiary structure followed by a change in the secondary structure as the guanidinium chloride concentration is increased. The tryptophan intensity results of Pappa and Cass (1993), on the other hand, gave no indication of a three-stage unfolding process but, given their instrumental settings, i.e., 290-nm excitation and 350-nm observation (vide supra), the third stage may have been obscured. Our results, obtained upon excitation at 295 nm and observation of the total emission intensity, indicate that the intrinsic tryptophan fluorescence of apoHRP correlates with the aforementioned CD data. Our lifetime and polarization results also indicate at least three stages in the unfolding process.

An issue related to discussions of apoHRP denaturation is the effect of hemin or PPIX on stabilization of the protein matrix. Our previous time-resolved fluorescence studies on apoHRP-PPIX (Jullian et al., 1989; Vargas et al., 1991; Brunet and Pulgar, 1993; Brunet et al., 1994) clearly demonstrated that the PPIX moiety is held very rigidly in the heme-binding site, which contradicts the assumption of Pappa and Cass (based on polarization data, which were not presented) that PPIX has "substantial mobility when bound to the protein" (Pappa and Cass, 1993). Pappa and Cass also reported that the denaturation profile of apoHRP-PPIX, followed by tryptophan fluorescence, was very similar to that of apoHRP and concluded that PPIX in the active site does not stabilize the protein as well as hemin. Our previous results, however, demonstrated that PPIX does indeed stabilize the protein matrix as well as hemin (Vargas et al., 1991).

The application of fluorescence methods to the study of proteins was initiated by Gregorio Weber. This study of the intrinsic fluorescence of apohorseradish peroxidase is a continuation of Gregorio Weber's legacy in several regards. First, the original study of the fluorescence of heme proteins, including horseradish peroxidase, was carried out by Weber and Teale in 1959. Second, all authors of this paper were either personally trained or strongly influenced by Gregorio Weber. Third, the results presented in this paper were discussed with Gregorio Weber, who offered many valuable insights. This paper is dedicated to the memory of Gregorio Weber, whose contributions to biological fluorescence and protein chemistry were both numerous and profound, and whose human qualities had such a powerful influence on generations of scientists.

We thank Dr. Theodore Hazlett and Dr. Tim Fulmer for their assistance with the lifetime and CD measurements and for helpful discussions.

This work was supported in part by National Science Foundation grant INT-930383 (DMJ), FONDECYT Chile grant 1930731 (JEB), and Universidad Católica de Valparaiso Institutional grants (JEB). ML acknowledges a CONICYT doctoral fellowship, and EG acknowledges National Institutes of Health grant RR03155.

## REFERENCES

Alcala, J. R., E. Gratton, and D. M. Jameson. 1985. Multifrequency phase fluorometry using the harmonic content of a mode-locked laser. *Anal. Instrum.* 14:225–250.

Alcala, J. R., E. Gratton, and F. J. Prendergast. 1987a. Resolvability of fluorescence lifetime distributions. *Biophys. J.* 51:587–596.

Alcala, J. R., E. Gratton, and F. J. Prendergast. 1987b. Fluorescence lifetime distributions in proteins. *Biophys. J.* 51:597–604.

Alcala, J. R., E. Gratton, and F. J. Prendergast. 1987c. Interpretation of fluorescence decay in proteins using continuous lifetime distributions. *Biophys. J.* 51:925–936.

Bartonek-Roxå, E., and H. Eriksson. 1994. Expression of a neutral horseradish peroxidase in *Escherichia coli*. *J. Biotechnol.* 37:133–142.

Bartonek-Roxå, E., H. Eriksson, and B. Mattiasson. 1991. The cDNA sequence of a neutral horseradish peroxidase. *Biochim. Biophys. Acta.* 1088:245–250.

Bismuto, E., E. Gratton, and G. Irace. 1988. Effect of unfolding on the tryptophanyl fluorescence lifetime distribution in apomyoglobin. *Biochemistry.* 27:2132–2136.

Brunet, J. E., G. A. Gonzalez, and C. P. Sotomayor. 1983. Intramolecular tryptophan heme energy transfer in horseradish peroxidase. *Photochem. Photobiol.* 38:253–254.

Brunet, J. E., and M. Pulgar. 1993. Dynamics of protoporphyrin IX in the heme pocket of horseradish peroxidase. *Biochim. Biophys. Acta.* 1203: 171–174.

Brunet, J. E., V. Vargas, E. Gratton, and D. M. Jameson. 1994. Hydrodynamics of horseradish peroxidase revealed by global analysis of multiple fluorescence probes. *Biophys. J.* 66:446–453.

Clarke, J., and L. M. Shannon. 1976. The isolation and characterization of the glycopeptides from horseradish peroxidase isoenzymes C. *Biochim. Biophys. Acta.* 421:428–442.

Das, T. K., and S. Mazumdar. 1995. pH-Induced conformational perturbation in horseradish peroxidase. Picosecond tryptophan fluorescence studies on native and cyanide-modified enzymes. *Eur. J. Biochem.* 227:823–828.

Delincee, H., and J. B. Radolla. 1970. Thin-layer isoelectric focusing on Sephadex layers of horseradish peroxidase. *Biochim. Biophys. Acta.* 200:3607–3617.

Eftink, M. R. 1994. The use of fluorescence methods to monitor unfolding transitions in proteins. *Biophys. J.* 66:482–501.

Gratton, E., D. M. Jameson, N. Rosato, and G. Weber. 1984. A multifrequency cross-correlation phase fluorometer using synchrotron radiation. *Rev. Sci. Instrum.* 55:486–494.

Gratton, E., N. Silva, G. Mei, N. Rosato, I. Savani, and A. Finazzi-Agro. 1992. Fluorescence lifetime distribution of folded and unfolded proteins. *Int. J. Quant. Chem.* 42:1479–1489.

Hartman, C., and P. R. Ortiz de Montellano. 1992. Baculovirus expression and characterization of catalytically active horseradish peroxidase. *Arch. Biochem. Biophys.* 297:61–72.

James, E. P. G., W. Wu, L. Stites, and L. Brand. 1992. Compact denatured state of a staphylococcal nuclease mutant by guanidinium as determined by resonance energy transfer. *Biochemistry.* 31:10217–10225.

Jameson, D. M. 1984. Fluorescence: principles, methodologies, and applications. *In* Fluorescein Hapten: An Immunological Probe. E. Voss, Jr., editor. Uniscience Series. CRC Press, Boca Raton, FL. 23–48.

Jameson, D. M., E. Gratton, and R. D. Hall. 1984. The measurement and analysis of heterogeneous emission by multifrequency phase and modulation fluorometry. *Appl. Spectrosc. Rev.* 20:55–105.

Jameson, D. M., and T. L. Hazlett. 1991. Time-resolved fluorescence in biology and biochemistry. *In* Biophysical and Biochemical Aspects of Fluorescence Spectroscopy. G. Dewey, editor. Plenum Press, New York. 105–133.

Jiskoot, W., V. Hlady, J. J. Naleway, and J. N. Herron. 1995. Application of fluorescence spectroscopy for determining the structure and function of proteins. *In* Physical Methods to Characterize Pharmaceutical Proteins. J. N. Herron, W. Jiskoot, and D. J. A. Crommelin, editors. Plenum Press, New York. 1–63.

Jullian, C., J. E. Brunet, V. Thomas, and D. M. Jameson. 1989. Time-resolved fluorescence studies on protoporphyrin IX-apohorseradish peroxidase. *Biochim. Biophys. Acta.* 997:206–210.

Mei, G., N. Rosato, N. Silva, R. Rusch, E. Gratton, I. Savini, and A. Finazzi-Agro. 1992. Denaturation of human Cu/Zn superoxide dismutase by guanidine hydrochloride: a dynamic fluorescence study. *Biochemistry.* 31:7224–7230.

Moosavi-Movajedi, A. A., and K. Nazari. 1995. Denaturation of horseradish peroxidase with urea and guanidine hydrochloride. *Int. J. Biol. Macromol.* 17:43–46.

Ohlsson, P. I., T. Horie, J. M. Vanderkooi, and K. G. Paul. 1986. Tryptophan in horseradish peroxidase. *Acta Chem. Scand.* B40:257–261.

Pappa, H. S., and A. E. G. Cass. 1993. A step towards understanding the folding mechanism of horseradish peroxidase. *Eur. J. Biochem.* 212: 227–235.

Paul, K. G., and T. Stigbrand. 1970. Four isoperoxidases from horseradish root. *Acta Chem. Scand.* 24:3607–3617.

Shannon, L. M., E. Kay, and J. Y. Lew. 1966. Peroxidase isoenzymes from horseradish roots. *J. Biol. Chem.* 241:2166–2172.

Silva, N., G. Mei, and E. Gratton. 1994. Protein fluorescence and conformational substates: the dynamics of human superoxide dismutase. *Comm. Mol. Cell. Biophys.* 8:217–242.

Smith, A. T., N. Santana, S. Dacey, M. Edwards, R. C. Bray, R. N. F. Thorneley, and J. F. Burke. 1990. Expression of a synthetic gene for horseradish peroxidase in *Escherichia coli* and folding and activation of

the recombinant enzyme with $Ca^{2+}$ and heme. *J. Biol. Chem.* 265: 13335–13343.

Spencer, R. D., and G. Weber. 1969. Measurements of subnanosecond fluorescence lifetimes with a cross-correlation phase fluorometer. *Ann. N.Y. Acad. Sci.* 158:361–376.

Spencer, R. D., and G. Weber. 1970. Influence of Brownian rotations and energy transfer upon the measurements of fluorescence lifetimes. *J. Chem. Phys.* 52:1654–1663.

Tamura, M., T. Asakura, and T. Yonetani. 1972. Heme-modification studies on horseradish peroxidase. *Biochim. Biophys. Acta.* 268: 292–304.

Teale, F. W. J. 1959. Cleavage of the heme-protein link by acid methylethylketone. *Biochim. Biophys. Acta.* 35:543.

Ugarova, N. N., A. P. Savitski, and I. V. Berezin. 1981. The protoporphyrin-apohorseradish complex as a horseradish peroxidase analog. A fluorimetric study of the heme pocket. *Biochim. Biophys. Acta.* 662: 210–219.

Vargas, V., J. E. Brunet, and D. M. Jameson. 1991. Oxygen diffusion near the heme binding site of horseradish peroxidase. *Biochem. Biophys. Res. Commun.* 178:104–109.

Watanabe, F., D. M. Jameson, and K. Uyeda. 1996. Enzymatic and fluorescence studies of four single-tryptophan mutants of rat testis fructose 6-phosphate, 2-kinase: fructose 2,6-bisphosphatase. *Protein Sci.* 5:904–913.

Weber, G. 1960. Fluorescence polarization spectrum and electronic energy transfer in proteins. *Biochem. J.* 75:345–352.

Weber, G., and F. W. J. Teale. 1959. Electronic energy transfer in haem proteins. *Disc. Faraday Soc.* 27:134–141.

Welinder, K. G. 1979. Amino acid sequence studies of horseradish peroxidase. *Eur. J. Biochem.* 96:483–502.

Welinder, K. G. 1985. Plant peroxidases. Their primary, secondary and tertiary structures and relation to cytochrome c peroxidase. *Eur. J. Biochem.* 151:497–504.